AD-A108 153 AIR FORCE GEOPHYSICS LAB HANSCOM AFB MA F/G 8/7
SEISMIC VELOCITY MODELS FOR WESTERN ALLUVIAL BASINS.(U)
MAY 81 J C BATTIS
UNCLASSIFIED AFGL-TR-81-0139 NL

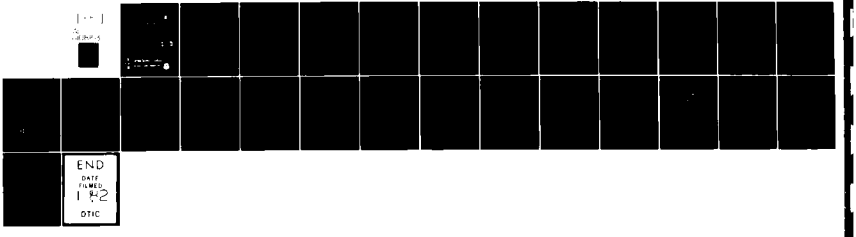

END
DATE FILMED
1 82
DTIC

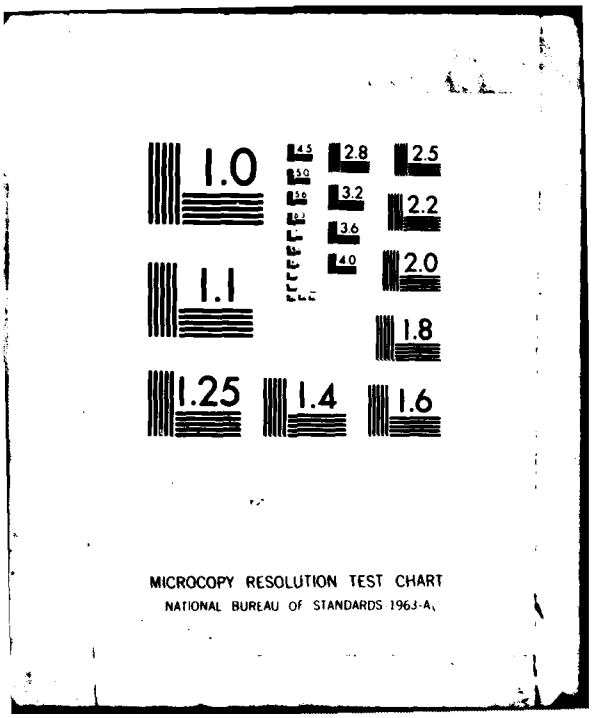
1.0
1.1
1.25
1.4
1.6
1.8
2.0
2.2
2.5
2.8
3.2
3.6
4.0
4.5
5.0
5.6
MICROCOPY RESOLUTION TEST CHART
NATIONAL BUREAU OF STANDARDS 1963-A

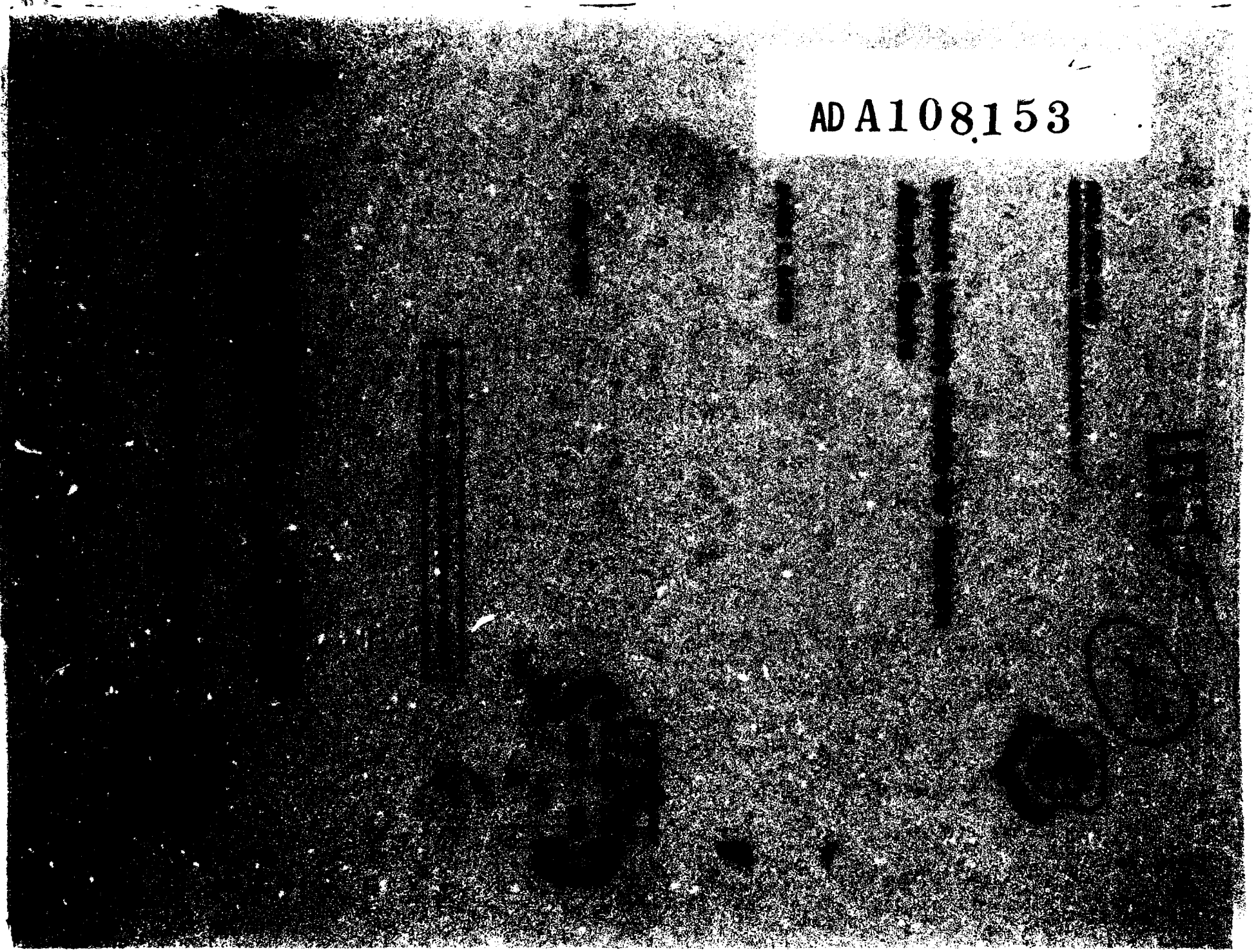

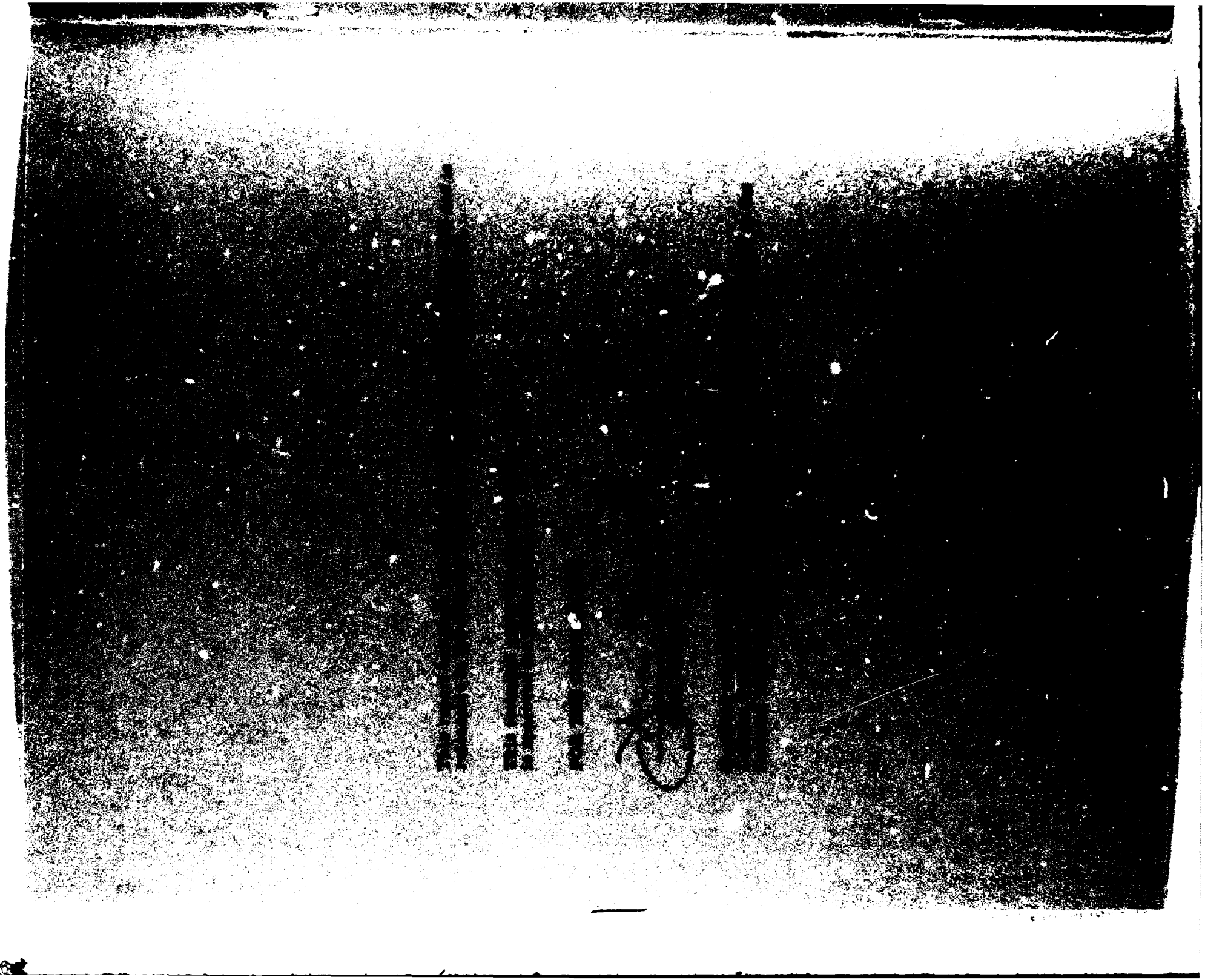

Unclassified
SECURITY CLASSIFICATION OF THIS PAGE (When Data Entered)

| REPORT DOCUMENTATION PAGE | | READ INSTRUCTIONS BEFORE COMPLETING FORM |
|---|---|---|
| 1. REPORT NUMBER<br>AFGL-TR-81-0139 | 2. GOVT ACCESSION NO.<br>AD-A109153 | 3. RECIPIENT'S CATALOG NUMBER |
| 4. TITLE (and Subtitle)<br>SEISMIC VELOCITY MODELS FOR WESTERN ALLUVIAL BASINS | | 5. TYPE OF REPORT & PERIOD COVERED<br>Scientific. Interim. |
| | | 6. PERFORMING ORG. REPORT NUMBER<br>ERP No. 740 |
| 7. AUTHOR(s)<br>James C. Battis | | 8. CONTRACT OR GRANT NUMBER(s) |
| 9. PERFORMING ORGANIZATION NAME AND ADDRESS<br>Air Force Geophysics Laboratory (LWH)<br>Hanscom AFB<br>Massachusetts 01731 | | 10. PROGRAM ELEMENT, PROJECT, TASK AREA & WORK UNIT NUMBERS<br>61102F<br>2309G202 |
| 11. CONTROLLING OFFICE NAME AND ADDRESS<br>Air Force Geophysics Laboratory (LWH)<br>Hanscom AFB<br>Massachusetts 01731 | | 12. REPORT DATE<br>5 May 1981 |
| | | 13. NUMBER OF PAGES<br>26 |
| 14. MONITORING AGENCY NAME & ADDRESS(if different from Controlling Office) | | 15. SECURITY CLASS. (of this report)<br>Unclassified |
| | | 15a. DECLASSIFICATION/DOWNGRADING SCHEDULE |

16. DISTRIBUTION STATEMENT (of this Report)

Approved for public release; distribution unlimited.

17. DISTRIBUTION STATEMENT (of the abstract entered in Block 20, if different from Report)

18. SUPPLEMENTARY NOTES

19. KEY WORDS (Continue on reverse side if necessary and identify by block number)

Alluvial basins
Basin and range
Seismic velocity
Velocity models
Crustal models

20. ABSTRACT (Continue on reverse side if necessary and identify by block number)

A study was made of the open literature on the geologic structure of the Basin and Range Province of the western United States. Based on this study, an attempt was made to derive a model of a typical basin for use in estimating the seismic ground motion characteristics of alluvial basins in the designated MX deployment area. Among the topics investigated are dimensions and structure of an average basin and characteristic seismic velocities in the basin interiors. In addition, many of the basins are expected to show significant variations from a typical structure and these variations are discussed.

DD FORM 1 JAN 73 1473

SECURITY CLASSIFICATION OF THIS PAGE (When Data Entered)

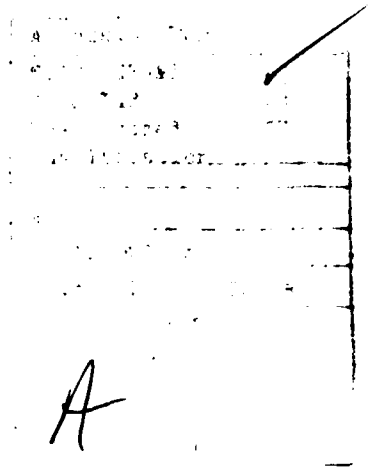

## Contents



## Illustrations

## Illustrations



## Tables

# Seismic Velocity Models for Western Alluvial Basins

## 1. INTRODUCTION

One geokinetic environment to which the MX Missile System could be subjected is strong ground motions at the deployment sites induced by earthquakes or explosive sources occurring at moderate distances from the sites of interest. The seismicity of the Basin and Range Province of Utah and Nevada, the designated deployment area, is sufficiently high that the effects of earthquake induced motions must be considered a realizable threat to the operational status of the missile system. A second source, the explosion, would be the result of either a large targeting error, or the direct attack on a different installation from the site being considered.

As direct measurement of the induced motions for either situation is unlikely, an understanding of these environments must rely on the prediction of the induced ground motions at the specific deployment sites based on mathematical source and seismic propagation models. For the deployment area, the prediction process is complicated by the shallow crustal structure of the region. Both analytical and empirical studies indicate that local seismic wave propagation in the Basin and Range Province cannot be modeled adequately using the typical simplifying assumptions such as plane layered crustal structure.

The use of more complex analytical procedures, such as three dimensional finite element or ray tracing analysis, requires models of the geologic structure

(Received for publication 5 May 1981)

through which the seismic waves will pass. In the following report, the structure of a typical basin is developed. Though each particular deployment basin can be expected to exhibit unique characteristics that will affect the propagation within that basin, it is expected that analysis of a general basin structure will provide significant insight into the important factors that determine ground motion.

## 2. REGIONAL GEOLOGY AND CRUSTAL STRUCTURE

The designated deployment sites for the MX Missile System are located in the Basin and Range Province of the western United States; more specifically, in central and eastern Nevada and western Utah (Figure 1). The primary topographic feature of the deployment region is a system of parallel and elongate basins separated by narrow mountain ranges. Erosion of the boundary ranges has resulted in extensive alluvial deposition within the basins. In addition, the development of the basin system has been accompanied by widespread volcanic activity, including basaltic diking and flow formation and ash deposition. The resulting complex basin structures, involving sharp velocity contrasts in three dimensions, are expected to have significant effects on the characteristics of local seismic wave propagation.

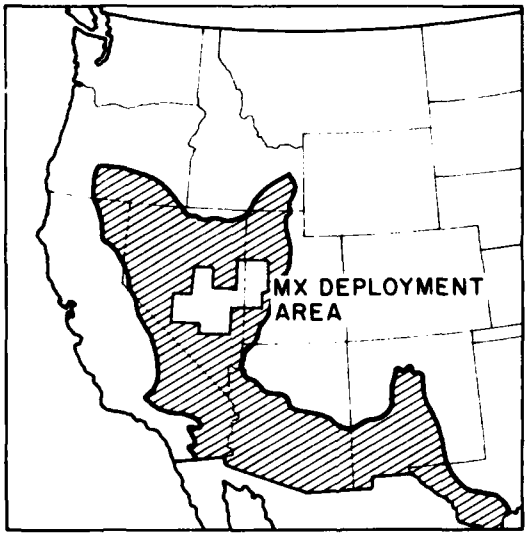


**Figure 1. Basin and Range Province (cross-hatched) of the Western United States and Designated MX Missile Deployment Area**

The primary tectonic process in the Basin and Range Province during the past 30 million years has been the lateral extension of the crust. Associated with this process, whether as cause or effect, was an epeirogenic uplift of the region. The tensional forces have been applied to the crust of this region since the late Cenozoic and have continued episodically to the present day.[1] During this period, the location and orientation of the active extension has varied within the province in apparent response to the changing mechanical relationship between the three crustal plates forming the Pacific margin of the United States: the North American, the Farallon, and the Pacific. In the area of interest, the present day landforms were generated by tensional forces oriented in an essentially east-west direction. These structures, however, overlay remnant structures from prior extensional episodes and, in some cases, may be controlled by the older features.[1,2,3]

In terms of seismology, the most significant regional features of the Basin and Range Province are an anomalous thin crust and pronounced low velocity zone in the upper mantle. These features are well-documented in several studies of the province.[4,5] In the deployment area, estimates of the crustal thickness range from 25 to 35 km. In contrast to the normal upper mantle P-wave velocity, $V_p$, of 8.2 km/sec, a velocity of approximately 7.6 km/sec was found.[5] In Figure 2, an average crustal structure for the deployment region is shown. Although not depicted in Figure 2, a thin region of slightly negative velocity gradient could form a lid on the low velocity upper mantle zone.[4] This velocity model is also given in Table 1. Shear wave velocities, $V_s$, for this model were obtained assuming the ratio $V_p/V_s$ equal to $\sqrt{3}$.

## 3. HORST AND GRABEN STRUCTURE

The dominant manifestation of the crustal extension in the Basin and Range Province is a system of normal faults which define the shallow crustal structure of the region (Figure 3). The pattern of faulting can be described roughly as


1. Eaton, G. P. (1979) A plate-tectonic model for late Cenozoic crustal spreading in the western United States, in Rio Grand Rift: Tectonics and Magmatism, R. E. Riecker, Ed., American Geophysical Union, Washington, D. C.
2. Kellogg, H. E. (1964) Cenozoic stratigraphy and structure of the southern Egan Range, Nevada, Geol. Soc. Am. Bull. 75:949-968.
3. Tweto, O. (1979) The Rio Grande Rift system in Colorado, in Rio Grand Rift: Tectonics and Magmatism, R. E. Riecker, Ed., American Geophysical Union, Washington, D. C.
4. Archambeau, C. B., Flinn, E. A., and Lambert, D. G. (1969) Fine structure of the upper mantle, J. Geophys. Res. 74:5825-5865.
5. Berg, J. W., Cook, K. L., Narans, H. D., and Dolan, W. M. (1960) Seismic investigation of the crustal structure in the eastern part of the Basin and Range province, Bull. Seism. Soc. Am. 50:511-535.

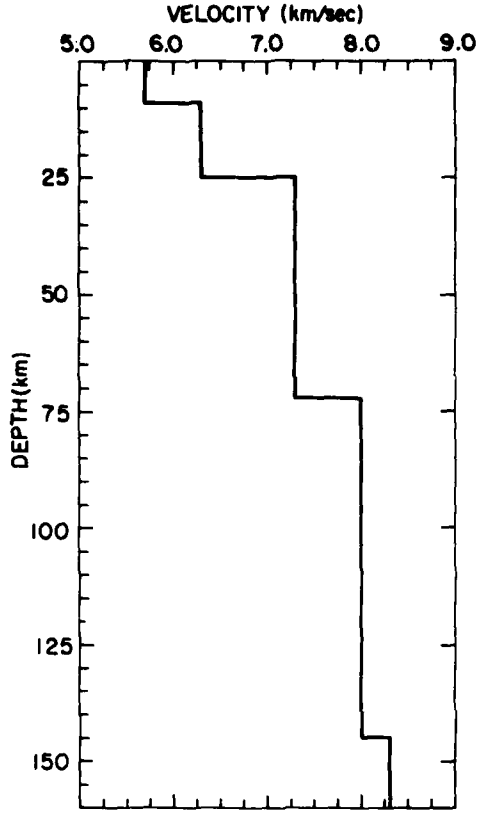


Figure 2. Crust and Upper Mantle P-Wave Velocity Structure for the Deployment Area

Table 1. Basin-Range Crustal Structure

| Layer | Thickness (km) | Depth (km) | $V_p$ (km/sec) | $V_S$ (km/sec) |
|---|---|---|---|---|
| 1 | 9 | 0 | 5.7 | 3.3 |
| 2 | 16 | 9 | 6.3 | 3.6 |
| 3 | 47 | 25 | 7.6 | 4.4 |
| 4 | 73 | 72 | 8.0 | 4.6 |
| 5 | ... | 145 | 8.3 | 4.8 |

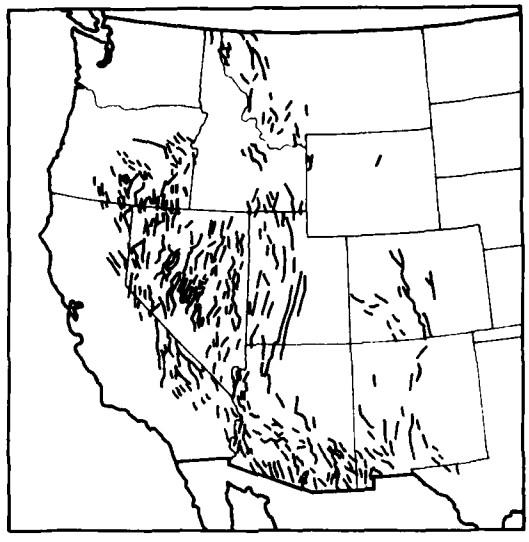

Figure 3. Cenozoic Normal Faults of the Western United States [After Gilluly (6)]

north-south trending parallel faults. Actually, the pattern is much more complex and approaches a rhombic structure when viewed in more detail than shown in Figure 3.[6] This system of faults could produce the alternating basin-range topography by either of two mechanisms. The first of these processes is the tilting or rotation of the crustal block lying between two listric faults as shown in Figure 4a. In this method, the elevated end of the block forms the range, whereas the depressed end forms the basin. In the second model (Figure 4b), the basin is defined by two normal faults of opposite dip. As the crust is extended, the central prism drops to form the basin. This mechanism produces a horst (relatively uplifted) and graben (relatively depressed) structural system. Most geophysical evidence supports the horst and graben model as the primary basin generation mechanism.[7] However, the tilting model may play a secondary role in the formation of some basins.

In addition to the bounding normal faults shown in Figure 4b, the central prism and alluvial fill are likely to be broken by additional subsidiary faults. The method by which the basins develop appears typically to involve numerous step

6. Gilluly, S. (1963) The tectonic evolution of the western United States, Quart. J. Geol. Soc. 119:133-74.

7. Stewart, J. H. (1971) Basin and Range structure: a system of horsts and grabens produced by deep-seated extension, Geol. Soc. Am. Bull. 82:1019-1044.

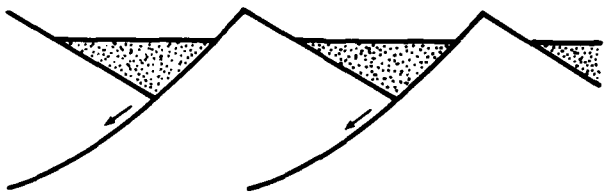

Figure 4a. Basin Formation by Crustal Block Rotation

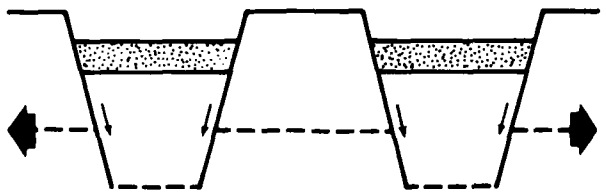

Figure 4b. Basin Formation by Normal Fault Motions (Large arrows represent extensional forces; small arrows indicate block motions)

faults rather than isolated displacements on the boundary faults.[7,8,9] A well-documented example of this structure is Dixie Valley (Figure 5) which, based on seismic refraction studies, shows this pattern of step faulting.[8]

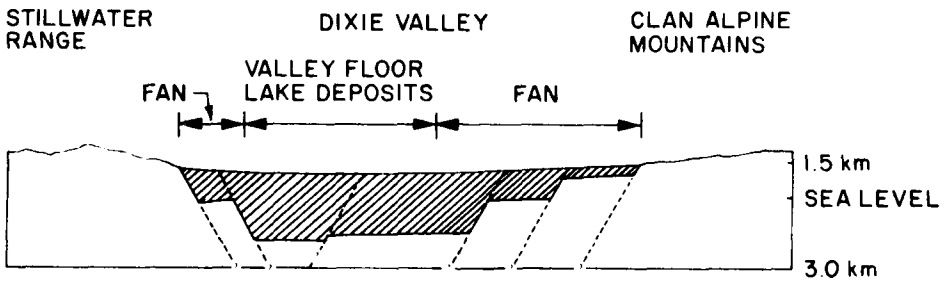


Figure 5. Generalized Cross Section of Dixie Valley [After Thompson (8)]

8. Thompson, G.A., Meister, L.J., Herring, A.T., Smith, T.E., Burke, D.B., Kovach, R.L., Burford, R.O., Salehi, I.A., and Wood, M.D. (1967) Geophysical Study of Basin-Range Structure: Dixie Valley Region, Nevada, Final Scientific Report AFCRL-66-848, Air Force Cambridge Research Laboratory, Hanscom AFB, Massachusetts.

9. Brown, L.D., Krumhansl, P.A., Chapin, C.E., Sanford, A.R., Cook, F.A., Kaufman, S., Oliver, J.E., and Schilt, F.S. (1979) COCORP seismic reflection studies of the Rio Grand Rift, in Rio Grand Rift: Tectonics and Magmatism, R.E. Riecker, Ed., American Geophysical Union, Washington, D.C.

The intrabasin faults, along with the boundary faults, are usually interpreted as high angle faults with dips in the range between 45° and 70° although shallower types do exist. Displacements are mostly dip-slip type motion with maximum throws on the order of several kilometers or more.[2] Sharp horizontal irregularities in the surface traces of most of these faults have been interpreted as restricting strike-slip motions. Continuing seismic activity within the deployment area indicates that many of these faults are still active, although the main areas of extension seem to be located at the fringes of the Basin and Range Province.[10, 1] However, it is unlikely that all are still active. As a consequence, it is expected that many of the faults detected in the basement rocks penetrate only part way through the basin fill.

A second feature of interest revealed in Figure 5 is the asymmetry of the graben structure. In the case of Dixie Valley, the deepest section of the basin is located to the west of the central axis. Whether the typical valley is symmetric or asymmetric is not well-established. It is apparent, however, that both forms can be found.[7] For the designated deployment area, topographic and gravity data indicate that most of the basins are symmetric, but a substantial number appear to be asymmetric (Figure 6).

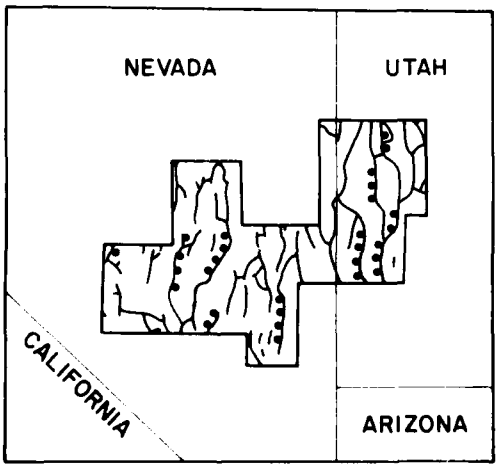


**Figure 6. Structurally Deepest Part or Center Lines of Grabens Within the MX Deployment Area. Apparent asymmetric grabens indicated by dots on side of shallowest bedrock slope [After Stewart (7)]**

10. Ryall, A. (1977) Earthquake hazard in the Nevada region, Bull. Seism. Soc. Am. 67:517-532.

Another form of asymmetry which may not be uncommon is the existence of minor horsts within the basins.[9] The structure of the basement, rather than being continuous, steps down into a single trough, which may involve a series of up and down steps with more than one trough in the basin. These horsts may reach the surface as intrabasin outcrops of basement rocks.

The termination of a graben is accomplished by progressively smaller vertical displacements on the generative fault systems. This mechanism is illustrated by the structure of northern Dixie Valley (Figure 7). The basement rock gradually shallows toward the ends of the valley. In a few cases, the terminus of the basin is defined by relatively steep slopes and the bounding mountain ranges on either side of the basin connect at elevations comparable with the remainder of the ranges. In the vast majority of cases, however, the terminus takes the form of a low pass through the boundary ranges and then opens into another basin; each basin can be seen as part of a connected system. Gravity data suggests that the axis of connecting basins tends to converge at high angles as would be expected for a deep seated extensional process.[7] This pattern is indicated in the centerlines of the basins in the MX deployment area (Figure 6).

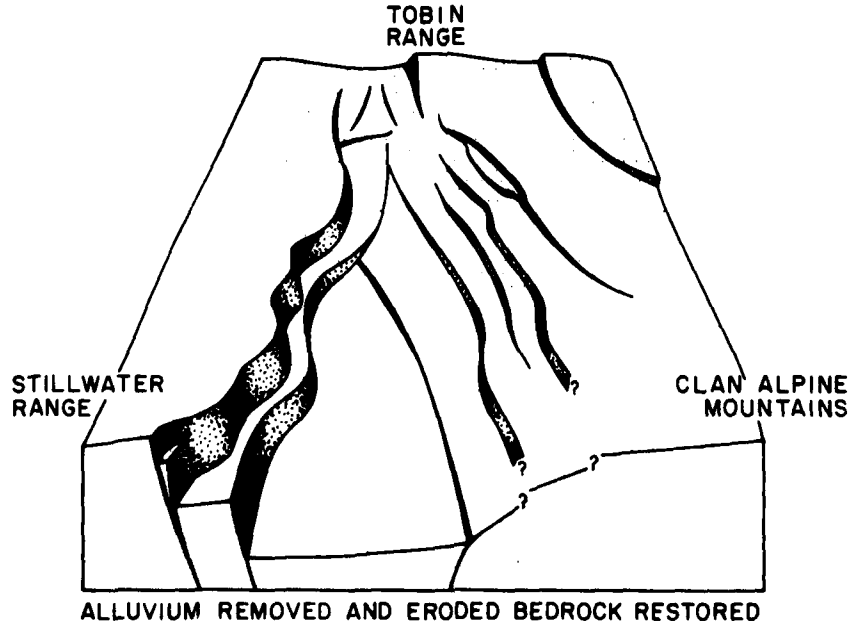


**Figure 7. Generalized Block Diagram of Central and Northern Dixie Valley Showing Basin Termination [After Thompson (8)]**

The dimensions of the graben structures are highly variable both from basin to basin and within a given valley. Approximate measurements were made of the designated deployment basins based on surface topography. From these measurements, dimensions of a typical graben were estimated. The width of most valleys tends to average between 15 to 20 km. However, many valleys have constrictions at which they narrow to about 5 km. The maximum diameters are usually less than 40 km. The lengths of the designated basins are highly variable and the estimation of this dimension is complicated by the interconnection of the basins, as described earlier. The lengths range from 20 km for Pahroc Valley, Nevada to approximately 150 km for Railroad and Spring Valleys, Nevada. Most of the siting basins have lengths in the vicinity of 70 km. The dimensions of the boundary mountain ranges are similar to those for the basins, typically 15 km wide. The elevation of the range ridgelines is between 300 and 1200 m above the alluvial floors of the valley.

The depth to the basement surface of grabens, or total depth of fill, can be determined by several geophysical surveying techniques, including gravity and seismic methods. Maximum depths vary from a few hundred meters in the smaller basins of western New Mexico to over 4000 m in the Albuquerque Basin.[11] These values are in agreement with determination made for basins in the Mojave, western Nevada and the Yuma Basin.[12,13] Crescent, Pine, Dixie, Smith Creer and Salt Well Valleys, all near but outside the designated deployment area, have maximum depths to basement in the range between 1000 and 3200 m, with an average value of about 2000 m.[7,8] It is assumed that this value would also be typical of basins in the deployment area owing to the proximity of these valleys.

The crustal blocks in which the grabens formed are composed of a diverse collection of rocks, including nonmarine sedimentary, volcanic and plutonic materials. This variety of rocks suggests a wide potential range for the basement and mountain range P-wave velocities. In the Yuma Basin, basement velocities of 4.3 to 5.5 km/sec were measured.[13] In situ velocity determinations of exposed bedrock in the Dixie Valley area gave estimates of 4.7 to 5.1 km/sec.[8] These

---

11. Seager, W.R., and Morgan, P. (1979) Rio Grande Rift in sourther New Mexico, west Texas and northern Chihuahua, in Rio Grande Rift: Tectonics and Magmatism, R.E. Riecker, Ed., American Geophysical Union, Washington, D.C.

12. Cabaniss, G.H. (1965) Geophysical studies of plays basins, in Geology, Mineralogy, and Hydrology of U.S. Playas, J.T. Neal, Ed., Air Force Cambridge Research Laboratories, Hanscom AFB, Massachusetts.

13. Mattick, R.E., Olmsted, F.H., and Zohdy, A.A.R. (1973) Geophysical Studies in the Yuma Area, Arizona and California, U.S.G.S. Professional Paper 726-D, Washington, D.C.

measurements suggest a typical bedrock velocity of 5.0 km/sec, in agreement with a model of Yucca Valley at the Nevada Test Site.[14]

For basement rock, the P-wave to S-wave velocity ratio can be assumed to be close to $\sqrt{3}$ or 1.73. This ratio implies an S-wave velocity for bedrock of 2.9 km/sec.

The similarity of rock types and seismic velocities between the Yuma Basin and those expected in the deployment area suggest a similarity in other physical properties, specifically density. Surficial samples of basement complex from the Yuma region are reported to have a range of densities from 2.4 to 2.9 g/cm$^3$.[13] A standard value of 2.67 g/cm$^3$ is used for topographic corrections in many gravity studies and is consistent with these values.

## 4. BASIN FILL STRUCTURE

As the graben structures developed, filling of the depressions was accomplished by two processes. The dominant mechanism has been the alluvial deposition of erosional products from the bounding mountain ranges. In addition, periods of volcanic activity in many of the basins produced significant ash and flow deposits. The resulting geologic structure within the basins is extremely complex and heterogeneous. Each of the designated deployment basins can be expected to exhibit a distinct structure that deviates significantly from any "typical" structural model. In this section, however, a first-order structural model is developed for use in the preliminary analysis of ground motions in alluvial basins.

The alluvial deposits found at the surface of most basins are representative of the types of material which would be found at depth. The surficial deposits can be divided into four basic morphological units: the alluvial fans, the bajada, the desert flats, and the playas or dry lakes. The alluvial fans are composed of poorly sorted and stratified detritus deposited by mountain streams as a result of the rapid decrease in slope as the streams enter the basins. Materials range from boulders to fine sand with a general decrease in particle size into the basin. The bajada is a transition zone between the fans and the desert flats. In this area, deposits of discreet fans intermix to form a zone of low slope consisting mostly of gravels to fine sands. The largest area of the basins generally is the desert flats, a region of low relief and shallow slope, composed mainly of sands and silts. The hydrological system of most basins is closed and during periods of high rainfall the lowpoints of the basins are flooded by formation of intermittent lakes. Evaporation of the lakes leave flat depositional beds of clay and silts that form the playas. Typical

14. Hadley, D.M., and Hart, R.S. (1979) Seismic Studies of the Nevada Test Site, Quarterly Technical Report SGI-R-79-003, Sierra Geophysics, Inc., Arcadia, California.

physical parameters for these surface deposits are given in Table 2. In Figure 8, expected ranges for the ratio $V_p/V_s$ for these materials are graphically presented.[15]

Table 2. Physical Properties of Surficial Basin Materials [Adapted from Ryall (10)]

| Seismic Velocities | | |
|---|---|---|
| Material | Velocity, m/sec | Landform Environment |
| Dry clay | 300 - 600 | Playa; desert flat |
| Moist clay | 850 - 1070 | Playa; (capillary fringe) Desert flat |
| Moist sand | 760 - 1070 | Desert flat (capillary fringe) |
| Saturated clay | 1525 - 1700 | Playa; groundwater discharging |
| Saturated sand | 1525 - 1550 | Desert flat; shallow $H_2O$ |
| Coarser alluvium | 1580 - 1650 | Bajada, fan |
| Boulder alluvium | 2470 | Fans, upper portion |
| **Density Values** | | |
| Material | $\rho$ (g/cm$^3$) | Landform |
| Dry clay | 1.20 - 1.45 | Playa; desert flat |
| Dry silt | 1.35 - 1.50 | Playa; desert flat |
| Moist clay | 1.60 - 1.80 | Playa, desert flat |
| Moist silt | 1.70 - 1.85 | Playa; desert flat |
| Saturated silt | 1.80 - 1.90 | Desert flat |
| Saturated sand | 2.15 | Desert flat, dunes |
| Dry alluvium | 1.60 - 2.00 | Fans, bajada |
| Wet alluvium | 2.15 - 2.30 | Fans; bajada |
| Compacted | 2.15 - 2.40 | Mixed, low porosity (fan/mat) - depth |

Cementation can increase density by as much as 20 percent and can double seismic velocity.

15. Paterson, N.R., and Meidav, T. (1965) Geophysical Methods in Highway Engineering, Paper presented at 48th Annual Convention of the Canadian Good Roads Association, Saskatoon, Saskatchewan.

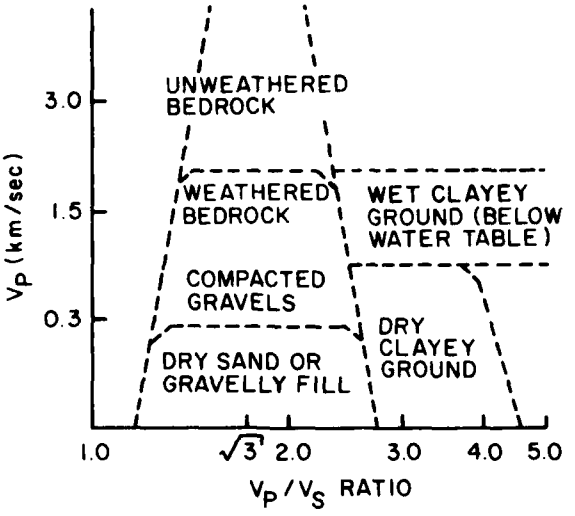


Figure 8. $V_p$ versus $V_p/V_s$ Ratio for Representative Materials [After Paterson and Meidav (15)]

Several factors, primarily weather, affect the areal extent of each type of deposit within the basins. Both short term and climatic variations result in complex interbedding of these units in the geologic column. In addition, alteration of physical properties due to cementation, overburden pressure and other processes produce substantial variations of the physical properties with depth. For the purposes of this study, the distribution of physical properties with depth is of more interest than the details of the basin layering.

The unique bedding expected within each basin and the lack of seismic models for basin fill in the literature make the development of a "standard" model difficult. A set of fifteen velocity models was assembled from the literature. Thirteen of these models are for sections of Dixie Valley and two are for Owens Valley, California.[8,16] This set was restricted to profiles for which bedrock velocities were observed. The layered models, given in Table 3, were divided into three groups, shallow (bedrock < 1250 m), intermediate (1250 m < bedrock < 2000 m), and deep sites (bedrock > 2000 m). These velocity profiles were derived from seismic refraction studies and provide only P-wave velocities. For each site classification and all sites taken together, an average velocity was evaluated at 10 m intervals. These velocity profiles are plotted in Figures 9 through 12. In addition, the absolute minimum and maximum velocity at each depth also are displayed.

16. Healy, J.H., and Press, F. (1964) Geophysical studies of Basin structures along the eastern front of the Sierra Nevada, California, Geophysics 29:337-359.

## Table 3. Alluvial Basin Models

Sources: DV - Dixie Valley
OV - Owens Valley

Class: S - Shallow
I - Intermediate
D - Deep

| Layer | Source: DV Class: I Thickness (meters) | Depth (meters) | Velocity (km/sec) |
|---|---|---|---|
| 1 | 15.0 | 0.0 | 0.7 |
| 2 | 27.0 | 15.0 | 1.6 |
| 3 | 155.0 | 42.0 | 1.9 |
| 4 | 265.0 | 197.0 | 2.4 |
| 5 | 1158.0 | 462.0 | 3.0 |
| 6 | 0.0 | 1620.0 | 4.7 |

| Layer | Source: DV Class: I Thickness (meters) | Depth (meters) | Velocity (km/sec) |
|---|---|---|---|
| 1 | 15.0 | 0.0 | 0.7 |
| 2 | 82.0 | 15.0 | 1.5 |
| 3 | 335.0 | 97.0 | 1.8 |
| 4 | 335.0 | 432.0 | 2.5 |
| 5 | 518.0 | 767.0 | 3.2 |
| 6 | 0.0 | 1285.0 | 4.8 |

| Layer | Source: DV Class: S Thickness (meters) | Depth (meters) | Velocity (km/sec) |
|---|---|---|---|
| 1 | 40.0 | 0.0 | 0.7 |
| 2 | 168.0 | 40.0 | 1.7 |
| 3 | 201.0 | 208.0 | 2.3 |
| 4 | 744.0 | 409.0 | 2.8 |
| 5 | 0.0 | 1153.0 | 4.8 |

| Layer | Source DV Class I Thickness (meters) | Depth (meters) | Velocity (km/sec) |
|---|---|---|---|
| 1 | 40.0 | 0.0 | 0.7 |
| 2 | 61.0 | 40.0 | 1.4 |
| 3 | 116.0 | 101.0 | 2.3 |
| 4 | 1006.0 | 217.0 | 2.8 |
| 5 | 305.0 | 1223.0 | 4.0 |
| 6 | 0.0 | 1528.0 | 4.9 |

| Layer | Source: DV Class: S Thickness (meters) | Depth (meters) | Velocity (md/sec) |
|---|---|---|---|
| 1 | 40.0 | 0.0 | 0.7 |
| 2 | 61.0 | 40.0 | 1.2 |
| 3 | 101.0 | 101.0 | 1.9 |
| 4 | 366.0 | 202.0 | 2.3 |
| 5 | 457.0 | 568.0 | 3.0 |
| 6 | 0.0 | 1025.0 | 5.1 |

| Layer | Source: DV Class: I Thickness (meters) | Depth (meters) | Velocity (km/sec) |
|---|---|---|---|
| 1 | 15.0 | 0.0 | 0.7 |
| 2 | 79.0 | 15.0 | 1.5 |
| 3 | 305.0 | 94.0 | 2.0 |
| 4 | 518.0 | 399.0 | 2.6 |
| 5 | 869.0 | 917.0 | 3.0 |
| 6 | 0.0 | 1786.0 | 4.9 |

| Layer | Source: DV Class D Thickness (meters) | Depth (meters) | Velocity (km/sec) |
|---|---|---|---|
| 1 | 10.0 | 0.0 | 0.7 |
| 2 | 76.0 | 10.0 | 1.5 |
| 3 | 335.0 | 86.0 | 1.9 |
| 4 | 518.0 | 421.0 | 2.5 |
| 5 | 1524.0 | 939.0 | 3.2 |
| 6 | 0.0 | 2463.0 | 4.8 |

| Layer | Source: DV Class: S Thickness (meters) | Depth (meters) | Velocity (km/sec) |
|---|---|---|---|
| 1 | 40.0 | 0.0 | 0.7 |
| 2 | 52.0 | 40.0 | 1.5 |
| 3 | 140.0 | 92.0 | 2.2 |
| 4 | 777.0 | 232.0 | 2.5 |
| 5 | 0.0 | 1009.0 | 4.5 |

| Layer | Source DV Class S Thickness (meters) | Depth (meters) | Velocity (km/sec) |
|---|---|---|---|
| 1 | 40.0 | 0.0 | 0.7 |
| 2 | 104.0 | 40.0 | 1.3 |
| 3 | 396.0 | 144.0 | 2.9 |
| 4 | 213.0 | 540.0 | 3.4 |
| 5 | 305.0 | 753.0 | 4.4 |
| 6 | 0.0 | 1058.0 | 4.9 |

| Layer | Source: DV Class S Thickness (meters) | Depth (meters) | Velocity (km/sec) |
|---|---|---|---|
| 1 | 40.0 | 0.0 | 0.7 |
| 2 | 34.0 | 40.0 | 1.4 |
| 3 | 134.0 | 74.0 | 2.2 |
| 4 | 805.0 | 208.0 | 2.7 |
| 5 | 0.0 | 1013.0 | 4.4 |

Table 3. Alluvial Basin Models (Cont.)

| Layer | Source DV Thickness (meters) | Class I Depth (meters) | Velocity (km/sec) |
|---|---|---|---|
| 1 | 15.0 | 0.0 | 0.7 |
| 2 | 335.0 | 15.0 | 1.7 |
| 3 | 488.0 | 350.0 | 2.1 |
| 4 | 366.0 | 838.0 | 3.0 |
| 5 | 791.0 | 1204.0 | 4.2 |
| 6 | 0.0 | 1995.0 | 6.3 |

| Layer | Source DV Thickness (meters) | Class D Depth (meters) | Velocity (km/sec) |
|---|---|---|---|
| 1 | 10.0 | 0.0 | 0.7 |
| 2 | 457.0 | 10.0 | 1.8 |
| 3 | 64.0 | 467.0 | 2.6 |
| 4 | 2134.0 | 531.0 | 3.2 |
| 5 | 0.0 | 2665.0 | 4.9 |

| Layer | Source OV Thickness (meters) | Class D Depth (meters) | Velocity (km/sec) |
|---|---|---|---|
| 1 | 161.0 | 0.0 | 1.5 |
| 2 | 781.0 | 161.0 | 2.4 |
| 3 | 1812.0 | 942.0 | 3.5 |
| 4 | 0.0 | 2754.0 | 4.7 |

| Layer | Source DV Thickness (meters) | Class D Depth (meters) | Velocity (km/sec) |
|---|---|---|---|
| 1 | 10.0 | 0.0 | 0.7 |
| 2 | 152.0 | 10.0 | 1.6 |
| 3 | 427.0 | 162.0 | 2.0 |
| 4 | 518.0 | 589.0 | 2.4 |
| 5 | 1036.0 | 1107.0 | 3.3 |
| 6 | 0.0 | 2143.0 | 6.3 |

| Layer | Source OV Thickness (meters) | Class S Depth (meters) | Velocity (km/sec) |
|---|---|---|---|
| 1 | 10.0 | 0.0 | 0.6 |
| 2 | 70.0 | 10.0 | 1.8 |
| 3 | 277.0 | 80.0 | 2.1 |
| 4 | 418.0 | 357.0 | 2.7 |
| 5 | 0.0 | 775.0 | 4.8 |

Velocity inversions which appear in these figures are actually artificial results of the averaging process. At the depth at which a model attained bedrock velocities, it was dropped from the averaging scheme. If the model was either contributing the maximum or higher than average velocity at this depth, the average or maximum velocity would appear to decrease for greater depths.

In Figure 13, the average velocity profiles for each site classification are plotted with the average profile for all sites showing the spread between these curves. While the observed range of velocities at each depth is as much as 3.0 km/sec, the average velocity profile is reasonably consistent for all three site classifications. It can be argued that the consistency results from the dominance of data from one basin. In Figure 14, the two Owens Valley profiles are plotted against the over-all average, showing good agreement with the average structure. Given the data available, it is felt that a layered model based on the average velocity profile for all sites is at least a first-order representation of a typical basin fill structure.

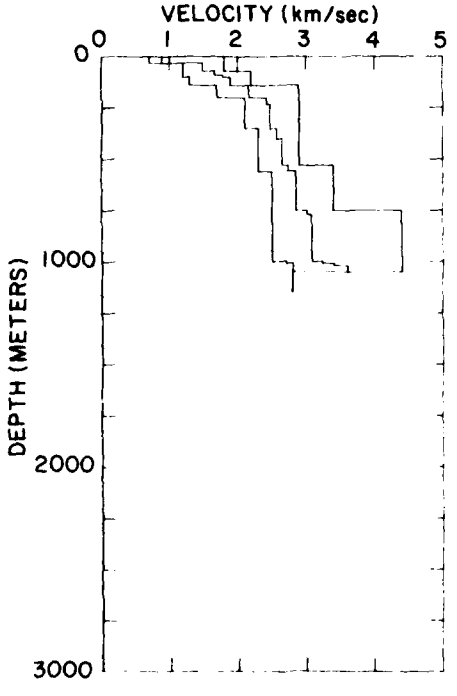


Figure 9. Average, Maximum and Minimum Velocity Profiles for Shallow Site Classification

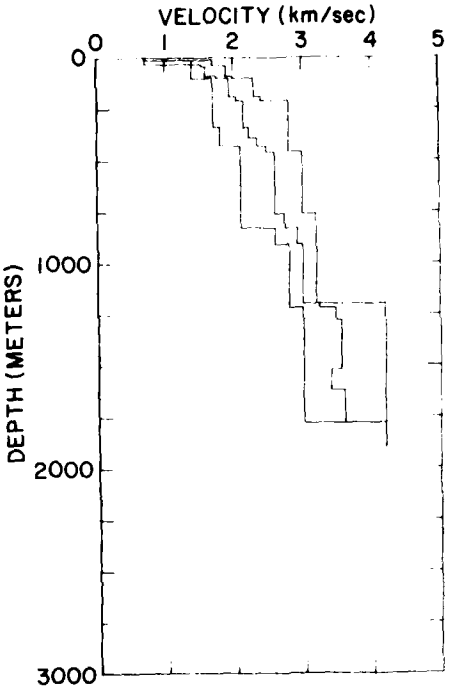


Figure 10. Average, Maximum and Minimum Velocity Profiles for Intermediate Site Classification

To obtain an S-wave velocity structure, an arbitrary relationship between depth and the ratio $V_p/V_s$, of the form:

$$V_p/V_s = 3.0 - 0.00317\ Z \qquad Z < 400\ m$$

and

$$V_p/V_s = \sqrt{3} \qquad Z > 400\ m$$

where Z is depth, was used to relate $V_p$ and $V_s$. The derived S-wave velocity profile, based on conversion of the P-wave velocity profile for all sites, is plotted

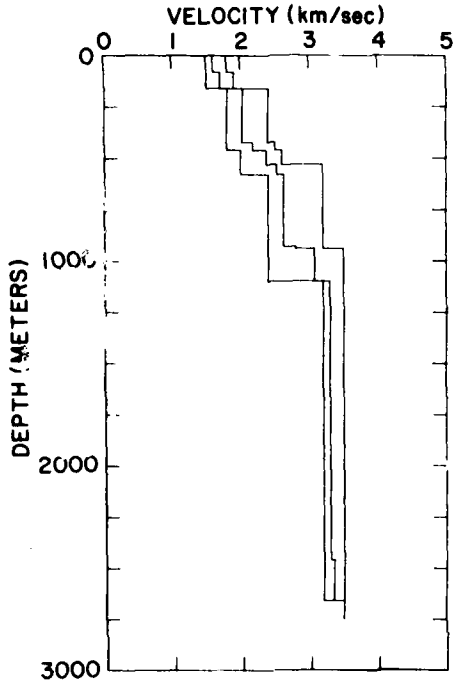


Figure 11. Average, Maximum and Minimum Velocity Profiles for Deep Site Classification

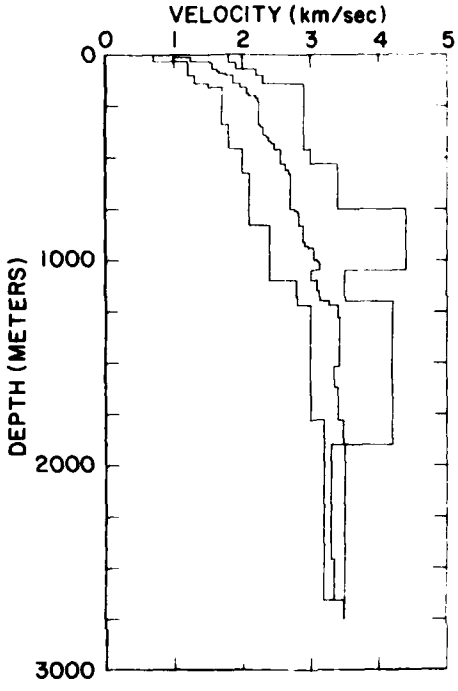


Figure 12. Average, Maximum and Minimum Velocity Profiles for All Sites

in Figure 15 against four S-wave velocity models for MX deployment basins evaluated by inversion of Rayleigh wave dispersion curves.[17] The derived $V_s$ profile appears to approximate an average of the empirical curves below 150 m. A better over-all fit could have been obtained by lowering the surface $V_p/V_s$ ratio of 3.0. This ratio was chosen so that the surficial S-wave velocity is less than the speed of sound in air as required to generate air-coupled surface waves which are expected in most alluvial basins. Although these data cover only the first 500 m,

17. Cherry, J.T., Farrell, W.E., Rodi, W.L., Swanger, H.J., and Shkoller, B. (1979) Shear Wave Velocities in MX Valleys Estimated from an Inversion of Rayleigh-Wave Group Velocities, Final Scientific Report SSS-R-80-4232, Systems, Science and Software, La Jolla, California

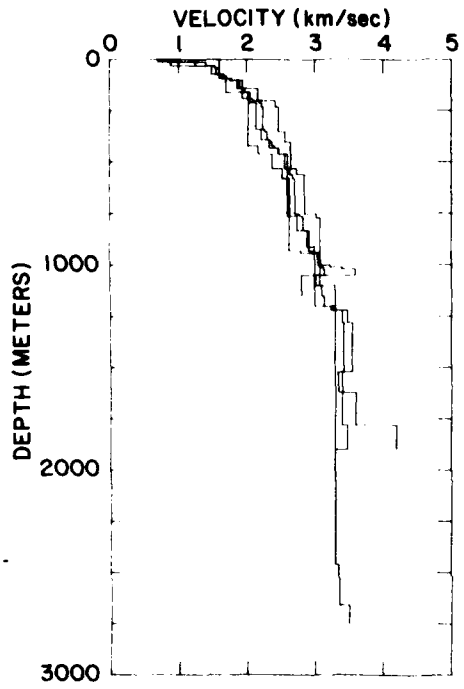


Figure 13. Average Velocity Profiles for Each Site Classification. All sites plotted to show small spread of average values

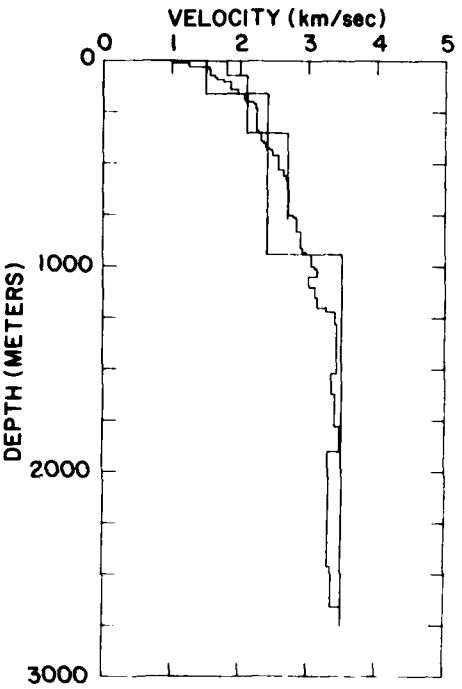


Figure 14. Average Velocity Profile Plotted Against the Two Owens Valley Velocity Models

the agreement between the derived and empirical curves tends to support the acceptability of this model as at least a first-order estimate.

In Table 4, the layered model used to approximate the average velocity curve is given. In Figure 16, this model is plotted against the average $V_p$ and $V_s$ curves.

Episodes of volcanic activity during basin formation have resulted in flow and dike formations and ash deposits and cones interbedded with the alluvial deposits. Volcanic deposits are typically located near the basin boundaries where normal faulting has produced zones of weakness along which intrusions have occurred. Surface flows, which may subsequently become buried, can extend well into the basin. An idealized example of the typical volcanic structure of basins is shown in Figure 17. The volcanic deposits can range from millimeters to hundreds of

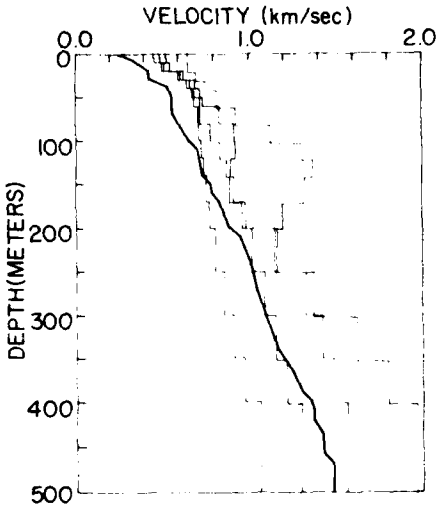


Figure 15. Derived S-Wave Velocity Profile Plotted Against Four S-Wave Velocity Profiles for MX Deployment Basins

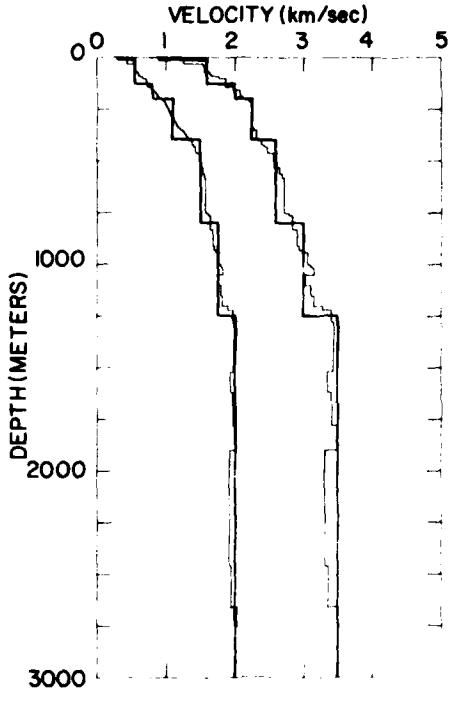


Figure 16. Average P-Wave Velocity Profile, Derived S-Wave Velocity Profile Plotted Against the Seven Layer Model for Basin Fill

Table 4. Basin Velocity Model

| Layer | Thickness (meters) | Depth (meters) | $V_p$ (km/sec) | $V_s$ (km/sec) |
|---|---|---|---|---|
| 1 | 10 | 0 | 0.9 | 0.3 |
| 2 | 115 | 10 | 1.6 | 0.55 |
| 3 | 75 | 125 | 2.0 | 0.8 |
| 4 | 200 | 200 | 2.25 | 1.1 |
| 5 | 400 | 400 | 6 | 1.5 |
| 6 | 450 | 800 | 3.0 | 1.75 |
| 7 | (to basement) | 1250 | 3.5 | 2.0 |
| 8 | ... | (basement) | 5.0 | 2.9 |

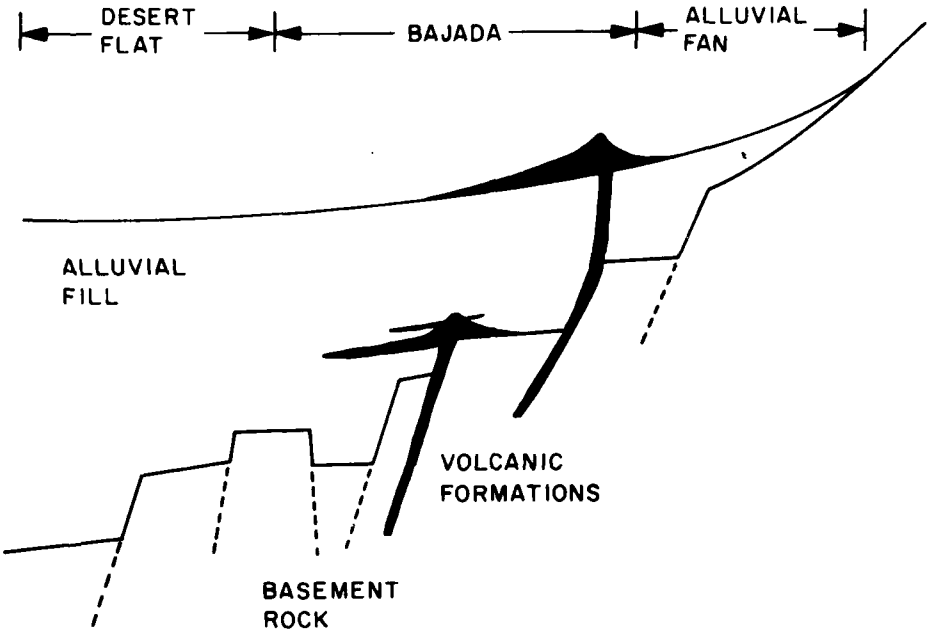


Figure 17. Volcanic Structures in an Idealized Alluvial Basin

meters thick and result in significant irregularities in the velocity profiles of the basin fill. Representative P-wave velocities of basalts and andesite, the major flow constituents, range from 5.0 to 6.5 km/sec.[18] Welded tuffs, a common ash deposit, have velocities of 1.6 to 5.5 km/sec, with an average velocity of about 2.8 km/sec for the P-wave.[19] Typical for basalt are S-wave velocities of 2.7 to 3.2 km/sec and 0.4 to 3.2 km/sec, with an average of 1.5 km/sec found for tuff. Either type of volcanic deposit has sufficiently high velocities to produce velocity inversions within the basin fill.

The variability of volcanic activity in each basin precludes the use of volcanic layers in a "typical model." The depth of the volcanic deposits can vary from surface deposits to any depth within the alluvial fill. These deposits can be ex-

18. Press, F. (1966) Seismic Velocities in Handbook of Physical Constants, S.P. Clark, Jr., ed., Geological Society of America.

19. Butters, S.W., Gronseth, J.M., and Patterson, J.F. (1980) Material Properties of Nevada Test Site Tuff and Grout, Final Scientific Report TR-80-35, Terra Tek, Inc., Salt Lake City, Utah.

pected to have a significant effect on the surficial ground motions. Preliminary modeling of seismic motions must examine cases in which velocity inversions occur.

## 5. CONCLUSION

Based on the data presented in the preceding sections, a first-order model for a "typical" MX deployment alluvial basin can be derived. The model basin is approximately 70 km in length with a width of 17 km. The maximum depth to bedrock within the valley is 2000 m. The basin is enclosed by mountain ranges which parallel the major axis. These ranges are about 15 km wide with an average elevation of 750 m above the base floor. A characteristic seismic velocity profile is given in Table 4. The available data suggests that the typical basin in the deployment region is symmetric.

However, the concept of a "typical" basin model is misleading. Within each basin, significant variations from the norm can be expected. For example, while most basins within the deployment region appear to be symmetric, a large percentage appear to be asymmetric. In addition, the occurrence of volcanic formations will be unique in each basin. In analyzing the seismic propagation characteristics of alluvial basins, one must consider both the typical model and variations on this model.

## References


1. Eaton, G. P. (1979) A plate-tectonic model for late Cenozoic crustal spreading in the western United States, in Rio Grand Rift: Tectonics and Magmatism, R. E. Riecker, Ed., American Geophysical Union, Washington, D.C.

2. Kellogg, H. E. (1964) Cenozoic stratigraphy and structure of the southern Egan Range, Nevada, Geol. Soc. Am. Bull. 75:949-968.

3. Tweto, O. (1979) The Rio Grand Rift system in Colorado, in Rio Grand Rift: Tectonics and Magmatism, R. E. Riecker, Ed., American Geophysical Union, Washington, D.C.

4. Archambeau, C. B., Flinn, E. A., and Lambert, D. G. (1969) Fine structure of the upper mantle, J. Geophys. Res. 74:5825-5865.

5. Berg, J. W., Cook, K. L., Narans, H. D., and Dolan, W. M. (1960) Seismic investigation of the crustal structure in the eastern part of the Basin and Range province, Bull. Seism. Soc. Am. 50:511-535.

6. Gilluly, S. (1963) The tectonic evolution of the western United States, Quart. J. Geol. Soc. 119:133-74.

7. Stewart, J. H. (1971) Basin and Range structure: a system of horsts and grabens produced by deep-seated extension, Geol. Soc. Am. Bull. 82:1019-1044.

8. Thompson, G. A., Meister, L. J., Herring, A. T., Smith, T. E., Burke, D. B., Kovach, R. L., Burford, R. O., Salehi, I. A., and Wood, M. D. (1967) Geophysical Study of Basin-Range Structure: Dixie Valley Region, Nevada, Final Scientific Report AFCRL-66-848, Air Force Cambridge Research Laboratory, Hanscom AFB, Massachusetts.

9. Brown, L. D., Krumhansl, P. A., Chapin, C. E., Sanford, A. R., Cook, F. A., Kaufman, S., Oliver, J. E., and Schilt, F. S. (1979) COCORP seismic reflection studies of the Rio Grand Rift, in Rio Grande Rift: Tectonics and Magmatism, R. E. Riecker, Ed., American Geophysical Union, Washington, D.C.

10. Ryall, A. (1977) Earthquake hazard in the Nevada region, Bull. Seism. Soc. Am. 67:517-532.

11. Seager, W.R., and Morgan, P. (1979) Rio Grande Rift in southern New Mexico, west Texas and northern Chihuahua, in Rio Grande Rift: Tectonics and Magmatism, R.E. Riecker, Ed., American Geophysical Union, Washington, D.C.

12. Cabaniss, G.H. (1965) Geophysical studies of playa basins, in Geology, Mineralogy, and Hydrology of U.S. Playas, J.T. Neal, Ed., Air Force Cambridge Research Laboratories, Hanscom AFB, Massachusetts.

13. Mattick, R.E., Olmsted, F.H., and Zohdy, A.A.R. (1973) Geophysical Studies in the Yuma Area, Arizona and California, U.S.G.S. Professional Paper 726-D, Washington, D.C.

14. Hadley, D.M., and Hart, R.S. (1979) Seismic Studies of the Nevada Test Site, Quarterly Technical Report SGI-R-79-003, Sierra Geophysics, Inc., Arcadia, California.

15. Paterson, N.R., and Meidav, T. (1965) Geophysical Methods in Highway Engineering, Paper presented at 48th Annual Convention of the Canadian Good Roads Association, Saskatoon, Saskatchewan.

16. Healy, J.H., and Press, F. (1964) Geophysical studies of Basin structures along the eastern front of the Sierra Nevada, California, Geophysics 29:337-359.

17. Cherry, J.T., Farrell, W.E., Rodi, W.L., Swanger, H.J., and Shkoller, B. (1979) Shear Wave Velocities in MX Valleys Estimated from an Inversion of Rayleigh-Wave Group Velocities, Final Scientific Report SSS-R-80-4232, Systems, Science and Software, La Jolla, California.

18. Press, F. (1966) Seismic Velocities in Handbook of Physical Constants, S.P. Clark, Jr., Ed., Geological Society of America.

19. Butters, S.W., Gronseth, J.M., and Patterson, J.F. (1980) Mechanical Properties of Nevada Test Site Tuff and Grout, Final Scientific Report TR-80-35, Terra Tek, Inc., Salt Lake City, Utah.

END

DATE
FILMED

1-82

DTIC